공학석사학위논문

나노제로그래피 기술의 향상을 위한 양하전된 절연체 위에서의 전기장 반전 과정에 대한 분석

Probing the Role of Electric Field Switching on a Positively Charged Dielectric Layer for Improving Nanoxerography

2015년 8월

서울대학교 대학원
기계항공공학부
이 해 욱

Probing the Role of Electric Field Switching on a Positively Charged Dielectric Layer for Improving Nanoxerography

Haewook Lee
Department of Mechanical and Aerospace Engineering
Seoul National University

Abstract

We report a new method to localize the high definition of surface charges on soft layers despite the use of the low levels of electric field by switching the voltages of an electrode contacted with a positively charged polymeric layer. During electrical contacts for nanoxerography, electric field switching was approached to control the electron and hole injection, leading to an anisotropic formation of charged regions with high definitions caused by the hole-blocking effect we found in the experiments. To verify this, depositions of charged nanoparticles and measurements of surface potential by Kelvin Force Microscopy (KFM) were carried out with a metal-coated hierarchical polymeric stamp. In the results, conditions for the direct writing of charges under a low level of electric field (< 4

V/㎛) were studied by increasing the initial level of positive ions coated onto a soft dielectric layer with the utilization of the electric field switching concepts, overcoming the limitation of an insufficient electrostatic focusing effect of charge patterns from the original nanoxerography.

Keywords : Nanoxerography, Electric Field Switching, Corona Charging, Dielectric, Charge Pattern, Nanoparticle Pattern

Student ID Number : 2013-23835

Contents

List of Figures

Figure 4.3 The results of 40-nm silver nanoparticle pattern through the present approach with the different positive ion deposition time.

Nomenclature

KFM	Kelvin Force Microscopy
AFM	Atomic Force Microscopy
SEM	Scanning Electron Microscope
ESP	Electrostatic Precipitator
DMA	Differential Mobility Analyzer
NP	Nanoparticle
$\triangle$V	Potential difference between inside and outside the charged region
V_{OUT}	Surface potential measured outside the charged region
V_{IN}	Surface potential measured inside the charged region
V_0	average initial values of surface potential elevated by the positive ion deposition

Chapter 1

Introduction

1. Introduction

Polymeric layers that featured both the facile trapping of electric charges and the localized inducing of dipoles[1] within the soft materials have been exploited in a wide range of applications such as photocopying, microphones[2], electrospinning[3], electret filters[4] and digital data storage[5] by applying a specific external electric field to the thin dielectric layer. In general, a variety of engineering techniques have been developed by adapting a concept of intrinsic inducing of the electric charges within the selected dielectric layer, to form an array of independently charged regions on soft polymeric materials. For the cases of the intrinsic localization with electric charges, studies employing high local electric field[6-8], contact electrification[9, 10], hot contact printing[11, 12] and even focused ion beam[13] have been mostly performed. However, severe damages on the weak and soft surface of polymers were potentially followed in compliance with the immoderate control of the experimental setup, partly owing to limitations in durability of the weak and soft materials. In parallel, facile and simple depositions by utilizing micro- or nano-substances with predefined charges were also carried out to avoid the aforementioned failures resulting from voltage breakdowns of the weak layers. To do this, various charged materials such as electrified liquids[14] and chemical substances[15] were tested via

coating-based extrinsic approaches, yielding a type of unwanted contaminations onto the target surface during the deposition process.

Nanoxerography is one of the well-established techniques toward a spatial distribution of local charges under a highly ordered and controlled manner with an aid of direct writing of electric charges, which obviously prevents the contamination of surfaces by employing a patterned electrode[6, 7, 16, 17] or a tip of atomic force microscopy (AFM) equipment[18, 19] for the process. Despite its simplicity and high definition of charged regions, however, there still remain some unresolved practical issues for the successful nanoxerography due to the fact that it requires excessive amounts of external field[20, 21] to trap electric charges on the soft layer as its origin lies in high accumulation of charges. Sometimes, it leads to a type of dielectric breakdown similar to the former intrinsic approaches (i.e. over 500 MV/m, in the case of ordinary polymers)[22]. Besides, the conventional nanoxerography techniques that consist of mere simple injections of electric charges showed potential lacks of possibilities for both introducing the initial charge concentration of trapped charges[23] and superposing the simultaneously induced dipoles[6]. Moreover, it is surely difficult to retain the localized region with introduced electric charges, especially from the low ranges of electric fields to avoid the breakdown of the polymer electrets.

To address these challenges, we present a simple, yet reliable

method to localize the electric charges via the nanoxerography by utilizing a type of electric field switching with the two-level hierarchical patterns as an array for individual conducting tips. The key idea is that the amplified injection of electrons[24] and the blocking of holes[25] were designed at the interface with positive ion coatings on the polymer surface. In the experiments, the sequential switching of external electric field further resulted in distinguishable differences in the charge levels compared to the background outside, after the field switching. Our switching-based strategy combines the injection of electric charges under a negative external potential in contact with the inducing of dipoles from a positive potentials after switching, allowing a facile and rapid localization of charges even at a quite low electric field range (< 4 V/㎛). To verify this, detailed measurements using a Kelvin Force Microscopy (KFM) and demonstrations with focusing of charged silver nanoparticles (NPs) via the charge patterns were performed, which could be used as a basic guide for localizing electric charges on the soft and weak polymer layers.

Chapter 2

Experimental

2.1 Preparation of the electrode and the substrate.

Two-level hierarchical polymeric electrode was prepared by using soft lithography[26-28] and metal coating (Pt) was followed as illustrated in Fig.2.1. The photoresist (AZ1512) was used as the polymer electret[29] where the surface charge pattern could be formed. The photoresist with the thickness of 1.2 ㎛ was spin-coated on a surface of thin dielectric layer of silicon dioxide (thickness ~ 100 nm) on a p-type (100) silicon wafer. The silicon was used as electrode during the next electric contacts, corona charging process and deposition process in the experiments.

2.2 Positive ion deposition by corona charging of the substrate

Corona discharge method[29] was carried out to produce the positive nitrogen ions. In the corona discharger, the tungsten needle was biased under 3.4 kV with the current of 0.005 mA and the positive nitrogen ions were generated by the discharge of the nitrogen gas supplied into the corona discharger under a flow rate of 3 L/min. The generated positive ions were fed into the grounded inlet of the electrostatic precipitator (ESP) chamber including the substrate with a deposition bias of −1.5 kV. The positive ions were accumulated on the surface of the substrate by the appropriate electric field in the ESP chamber and led to the formation of the positive surface charge before the electrical contacts process.

2.3 Generation and guidance of the singly and positively charged monodisperse nanoparticles

The singly charged silver nanoparticles were generated by an evaporation and condensation method and then classified to monodisperse nanoparticles utilizing a nano-Differential Mobility Analyzer (DMA, TSI 308500) and DMA controller (AERIS) after the particles had been charged in a neutralizer[30, 31]. For producing the silver nanoparticles, silver beads which had been put in a tube furnace at ~1,200 ℃ were evaporated and then delivered to a cooling tube at ~26 ℃ with the carrier gas of nitrogen. Through the process, polydisperse particles were generated and grown by condensation and coagulation process. In order to produce the singly charged monodisperse nanoparticles, silver nanoparticles were charged bipolarly in the neutralizer (HCT Aerosol Neutrailizer 4530) and sorted monodispersely in the DMA according to the electrical mobility of the charged nanoparticles. The singly charged monodisperse 40-nm nanoparticles were produced with a concentration of 2.0 X 10^6 cm^{-3}. These charged aerosols were fed to the ESP chamber that contained the substrate under a flow rate of 1.5 L/min for 20 minutes and positively charged aerosols were attracted toward the substrate with a deposition bias of -4 kV due to the

electrostatic force.

2.4 KFM measurements

KFM measurements of the surface potential on the substrate were performed with a XE-100 Kelvin Force Microscopy (Park Systems, Korea) at a scanning rate of 0.2 Hz over the area of 45 X 45 μm^2. In order to avoid the unnecessary decay of surface charges, the charged sample was placed on apparatus for KFM immediately after the end of each process including the corona charging and the electrical contact.

Chapter 3

Fabrication of charge patterns and deposition of positively charged nanoparticles

3.1 Fabrication of Charge Patterns

A schematic illustration for the process of nanoxerography and electric field switching is shown in Fig. 3.1, where three steps consisting of a positive ion deposition (a1), an electrical contact with negative bias from hierarchical electrodes (a2), and a sequential electric field switching (a3) are briefly described. It is very well-known that the conventional nanoxerography process employs only a direct writing of charges on the polymer layer under the negative bias (a2), which potentially generates a poor definition of electric charge accumulations on the surface when a low level of electric bias was applied to the sample. In the previous study[29], we reported that the introduction of positive ion coating prior to the nanoxerography could enhance the definition of induced charges due to the clarification between the charged regions (i.e., negative) compared to the remaining background (i.e., positive) after the process. In the meanwhile, we further found a new strategy that is based on a type of electric field switching (a3) to effectively reinforce the intensity of charges on a positively charged surface, which also gives an obvious opportunity for the fractal-like growth of charged NPs onto the soft surface with localized charges despite the use of quite low potentials during the electrical contacts. To write the charge patterns uniformly, the hierarchical polymeric stamp fabricated through the process as shown in Fig. 2.1, is utilized to

ensure a conformal contact[26] because the electrode–sample distance is a crucial factor for the injection of charges[20] in this approach. The details about these processes will be demonstrated with results of surface potential on the charge patterns measured by KFM in Fig. 3.3

3.2 Deposition of positively charged nanoparticles

When several charged NPs are delivered and placed onto the regions with localized charges as shown in the Fig. 3.1b, attractive forces are applied to each positively charged particle due to the negative bias from the substrate so that they could spontaneously be ahead to the soft surface in accordance with a type of focusing as an electrostatic lens[29]. The localized charge pattern is prone to generate a convex electrostatic lens owing to the potential differences (△V) around the region, leading to the clear contrast of the attracted NPs in the area. Note that the focusing performance in this study guarantees a good fidelity at the charged area even with much lower values of the external bias during a charge writing (−2 V and +4 V) after positive ion deposition of 30 min, while the soft surface under the conventional nanoxerography showed poor contrast with NPs that were also observed at the outside of the charged area although the conventional nanoxerography was performed under high voltage conditions (−400 V). According to the scanning electron microscopy (SEM) images in the Fig. 1c, there are a lot of individual NPs as noises in the background of the area (5 ㎛ in diameter) on the surface of a soft photoresist (AZ1512) with a thickness of 1.2 ㎛ although the inner area showed some agglomerated NPs in compliance with the focusing via an

electrostatic lens. In contrast, the noises could not be monitored in the case of the surface after the positive ion coating, together with the electric field switching, which indicates that a high definition of electrostatic lens was yielded even though the applied potential was quite low. In order to support the validity of the fabrication for charge patterns and focusing of the charged nanoparticles via the current method, various images are shown in Fig. 3.2. In the results, uniform formations of 40-nm silver nanoparticle patterns were allowed over large areas (5 X 5 mm^2), and the fractal structure or mesh were obtained on the substrate by using different shapes of the electrode such as 5-㎛ pillars or holes onto the cylinder of 150 ㎛ in diameter.

3.3 Detailed procedures for charge writings with the surface potential data measured by KFM

The overall process and detailed illustration are delineated in the Fig. 3.3a, in which both the positive ion neutralization and the polarization reversal[32] after the corona charging process play a key role for the effective localization of the charges after the field switching. Because of the pre-coated positive ions on the dielectric layer, the injection of electrons and holes could be controlled asymmetrically[24, 25] from the hierarchical electrode during the electric field switching process, resulting in the different mechanism to produce the charge patterns for the next two steps. After performing a short ion deposition (~ 5 sec), the next positive ion neutralization was followed by applying a negative bias (- 2 V) for 3 min to the surface by using the Pt-coated hierarchical stamps. During this period, electron injection happened on the top surface with positive ions under a conformal contact with the hierarchical electrodes, partially neutralizing the charge level of the pre-deposited positive ions, and leading to a small decrement in the surface potential. However, the area outside of the contacted region is not affected by the partial neutralization. The graph in Fig. 3.3b is the measured surface potentials at each stage of the surface

treatment. In the experiment, 7.17 V of average surface potential (green line in the Fig. 3.3b) was measured by using the KFM analysis, while some decrement in the potential level (~ 0.77 V) was detected after the positive ion neutralization (~ 6.40 V, blue line in the Fig. 3.3b). The small amount of decay was shown to come from the surface conduction or intrinsic conduction[33]. A careful inspection on the charged region reveals that there exists an unexpected drop of the potential level (~ 0.042 V) over the contacted region after the partial neutralization process as shown in the inset in Fig. 3.3b. It should be noted that the partial neutralization of the positive ions in response to the injected electrons in this study mainly affects the charging of the electrets, although another charging was also simultaneously originated, in part, from the polarization of dipoles inside the polymer film[6], resulting in the decrease in the surface potential at the region in contact with the 5 ㎛ electrode.

Next, we performed a type of polarization reversal procedure by switching the bias from negative to positive, for increasing the unexpected drop of potential levels under the each contacted region. According to the result, the average potential level was measured to decrease to approximately 0.45 V from blue line to red line in Fig. 3.3b due to the same effect from the decay after a moderate electrical contact (~3 min) with switched bias (+4 V) of the hierarchical electrode. However, the same procedure increases the potential drops onto the contacted region by 0.246

V, which means that the reinforcement of the pre-deposited charges resulted from a negative dipole polarization during the switching bias from −2 V to +4 V simultaneously while the injection of holes was inhibited and blocked at the positively charged surface[25].

Chapter 4

Probing the role of pre-coated positive ion and the electric field switching for improving nanoxerography

4.1 Probing the role of pre-coated positive ion and electric field switching with the results of nanoparticle patterns

As we previously mentioned relating to the potential drops during the electric contact on pre-coated positive ions, there are two different types of fundamental mechanisms for the charging of the polymer electrets[6]: (i) transferring the electrons or holes directly from the electrode during an electric contact under a specific bias, and (ii) inducing the dipoles from the internal field within the dielectric polymer layer. We designed the charge-injection experiments to set the effectiveness of the pre-coated positive ion and the field switching, apart from the results via both the conventional nanoxerography without positive ion coatings (Fig. 4.1a) and the nanoxerography with ion coatings (Fig. 4.1b), in order to elaborate the soundness of our approaches including positive ion coating and field switching processes (Fig. 4.1c). To check the tendencies on the charging of each case, a large amount of charged silver NPs (40 nm in geometric diameter) were prepared and monitored by placing them onto the charged surface, where they are directly guided via an array of electrostatic lens on the surface.

When the simple conventional nanoxerography without the ion coating was performed under a positive bias (+ 4 V) for 3 min,

most of the charged NPs were repelled out from the contacted region (5 ㎛ in diameter) as shown in the SEM image in Fig. 4.1a, since the charged and contacted region after nanoxerography displayed much higher electric potentials compared to the neighboring background as commonly known in other experiment[7]. The schematic illustration in the inset of Fig. 4.1a showed the corresponding potential lines on the charged surface, where the potential difference acts as the repelling force from the center region because the holes injected from the electrode with positive bias were trapped on the contacted polymer layer, though this same process also resulted in the inducing of dipoles negatively. On the other hand, the NPs were weakly and inversely collected near the center region in the contact with the positively biased electrode (+4 V) after simply employing the positive ion coatings on the polymer (Fig. 4.1b) because of the lowered electric potentials on the contacted region. This opposite focusing of NPs indicates that the pre-accumulated positive ions could be a barrier layer against the injected holes[25] and thereby dominant potential drop could be caused on the contacted region by the negative dipoles.

To exploit both the induced dipoles and injected charges for high definition of charges on the soft surface, we further verified a concept with electric field switching as shown in the Fig. 4.1c, in which negative bias (−2 V) was applied for 3 min to the surface prior to the contact with positive bias (+4 V) for the

switching concept, displaying the assembly of the fractal structure of silver nanoparticles. When the negative bias was applied to the positive ion-coated surface, the pre-deposited positive ions were partially neutralized during the time. In the meanwhile, dipoles were induced within the polymer layer from the external electric field, providing the slight decrement of potential levels (~ 0.042 V) on the surface from the superposition with the induced dipoles under the surface. Note that the partial neutralization could keep the positively charged ions remain on the area as a barrier for the holes during the injection of electrons via negative bias, whereas the same barrier prevents noticeable transport of holes after the bias switching. We applied positive bias (+4 V) as the switching, which obviously leads to the change of dipole moments within the polymer layer and reduces the surface potentials due to the polarization reversal. In this case, the potential difference showed much elevated values (~ 0.246 V) and demonstrated an effective attraction of the charged NPs in the contact area that has lowered potential compared to the values of surroundings. Thus, the electric field switching could further reduce the surface potentials to increase the potential difference at the given surface since the crucial role of the positive ions that could disturb the injection of the holes, suggesting the facile modulation of the potential levels via the switching of bias to form the highly attractive soft surface with charged ions as well

as the particle-assembled structures with the electrostatic lens arrays.

4.2 Probing the role of pre-coated positive ion for improving nanoxerography with the measurements of surface potential on charge patterns.

Owing to the simple modulation of injected charges and potential levels by using both the positive ion coating and the electric field switching on the soft polymer layers, direct writing of sufficient spatial electric charges is possible under the quite low value of electric fields (< 4 V/㎛), together with abilities to generate arrays with controlled charge densities. To approach this, we performed a series of experiments under the same condition of electric field switching process (−2 V and + 4 V) with samples having different levels of positive ion coatings, where the different levels of initial potential were measured after the deposition processes. The Fig. 4.2a depicts the independent four-cases of samples with surface potentials from 4.03 V to 2.56 V as average initial values (V_0) outside the region in contact with the 5 ㎛ electrode for the positive ion coatings. After performing same bias switching processes on each surface with different value of initial surface potential, we obtained the accelerated and increased potential drops on the contacted regions with the higher levels of pre-coated positive ions as shown in the Fig. 4.2b. In the results, the measured potential

drops were proportional to the initial potentials from 0.145 V to 0.098 V and there still exists the reasonable decrement of the potentials compared to the values on neighboring surfaces. The tendency is briefly shown in the Fig. 4.2c, suggesting that the modulation with increasing the initial surface potential is useful to enhance the intensity of the charged regions onto the surface as we intended. This is potentially possible from the improved effect of controlling the injection of the charges by increasing the positive ion concentration, which promotes the injection of electrons[24] but restricts the injection of holes[25], asymmetrically.

4.3 Probing the role of pre-coated positive ion for improving nanoxerography with the results of nanoparticle patterns.

This possibility was supported with the deposition results of the positively charged nanoparticles as shown in Fig. 4.3. When the positive ions was deposited for 30 min in advance, the designed charge pattern had the strong focusing effect that could not be obtained in the conventional nanoxerography due to the aforementioned problem and the same tendency equal to the Fig. 4.2c were shown with the different deposition time of the positive ions from 1 min to 30 min, enhancing the intensity of charge patterns with the increase in the deposition time of positive ions. However, almost same results of nanoparticle patterns were obtained as shown in Fig. 4.3(a1) and (c), which indicate the different positive ion deposition time of 30 min and 1 hour, because the increase in the positive ion concentration could be potentially limited to the saturation of the deposited positive ions on the substrate, demonstrating the maximum intensity of charge patterns could possibly exist through the new concept.

Chapter 5

Conclusion

5. Conclusion

In conclusion, we have presented a new strategy to overcome a lack of focusing effect of the charge patterns in the case of conventional nanoxerography by switching the voltages applied to the electrode onto the positively charged dielectric layer. Although the quite low range of electric field was applied to the polymeric layer (< 4 V/㎛), the present method surely enables uniform formations of both high definition of charges and particle assemblies with the enhanced focusing effect, assembling nanoparticles into the fractal structure. The pre-coated positive ion has the crucial role for our approach which includes two sequential processes of electrical contacts for producing charge patterns under both the negative and the positive electric field, promoting the injection of electrons but blocking the injection of holes unsymmetrically. The effect of the deposited positive ions was proved through the KFM measurement and from the focusing results of charged nanoparticles. Finally, it was demonstrated that the intensity of the designed charge patterns could be effectively enhanced by elevating the positive surface potential on the substrate despite the use of the fixed value of the applied electric field, localizing the high definition of charge patterns on the soft layers and resulting in the fractal assembly of the nanoparticles without the noises.

Figures

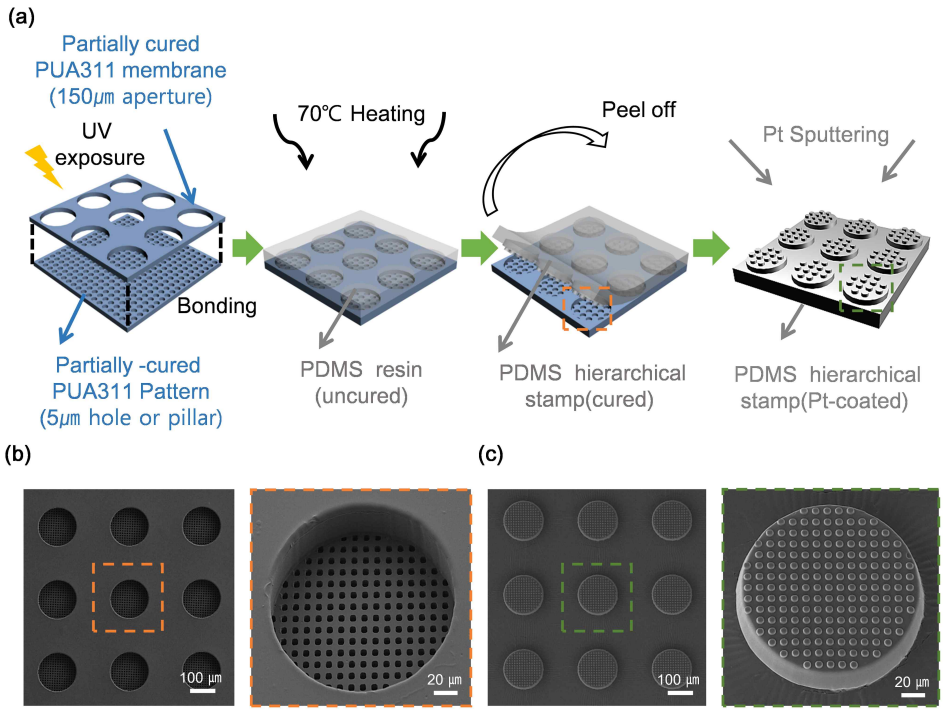

Figure. 2.1 (a) Illustration for the fabrication of a hierarchical conductive electrode. (b) SEM Images of a two-level multiscale mold (5/150 ㎛ in diameter, from bottom to top). (c) SEM Images of the hierarchical conductive electrode with coated platinum in the thickness of 20 nm after the replication from the two-level mold.

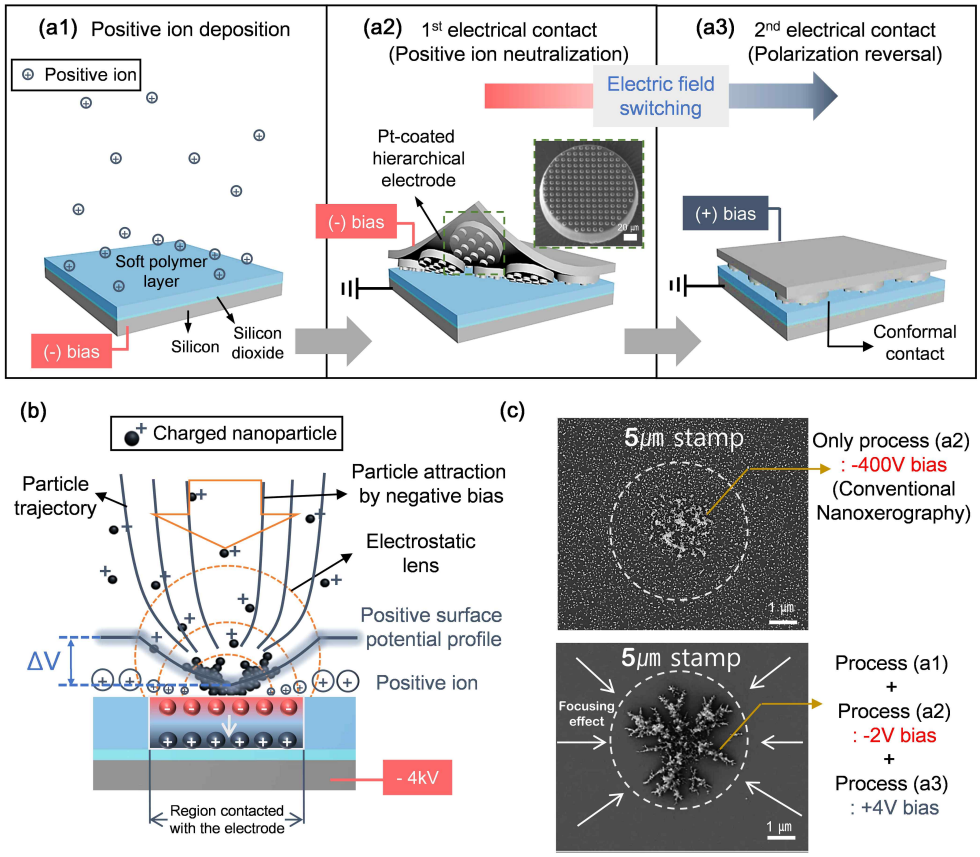

Figure 3.1. (a1–a3) Schematic diagram for generating charged regions through three–step processes. (a1) Positive ions are accumulated on a soft polymeric layer. (a2) A pre–patterned and metal–coated hierarchical electrode is positioned on the polymer and biased negatively. The inset shows a SEM Image of the two–level hierarchical electrodes (5 ㎛ pillars and 150 ㎛ dots, from top to bottom). (a3) The applied voltage is switched from negative to positive while in a conformal contact with the substrate. (b) Illustration for focusing positively charged

nanoparticles toward the center region contacted with the electrode via electrostatic lens. (c) SEM Images of three-dimensional assemblies produced by conventional nanoxerography (upper image) and present procedures (lower image).

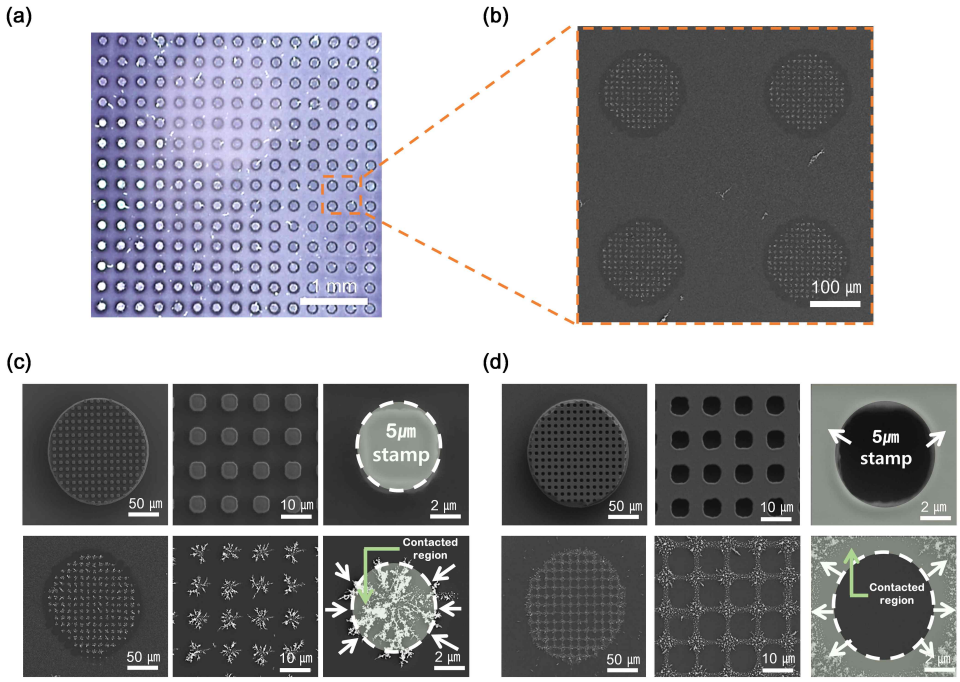

Figure 3.2 (a) An optical image of 40-nm silver nanoparticle patterns on the substrate produced through our concept utilizing the Pt-coated hierarchical electrode (5/150 μm in diameter, from top to bottom). (b) A SEM image of nanoparticle patterns including fractal structures inside each region of 150 μm in diameter. (c,d) SEM images of the utilized stamp and nanoparticle patterns. The array of fractal structures (**c**) or meshes (**d**) were patterned in the same array of the electrode such as 5-μm pillars or 5-μm holes, respectively on the 150-μm dots. The charged nanoparticles were focused into a region contacted with the electrode.

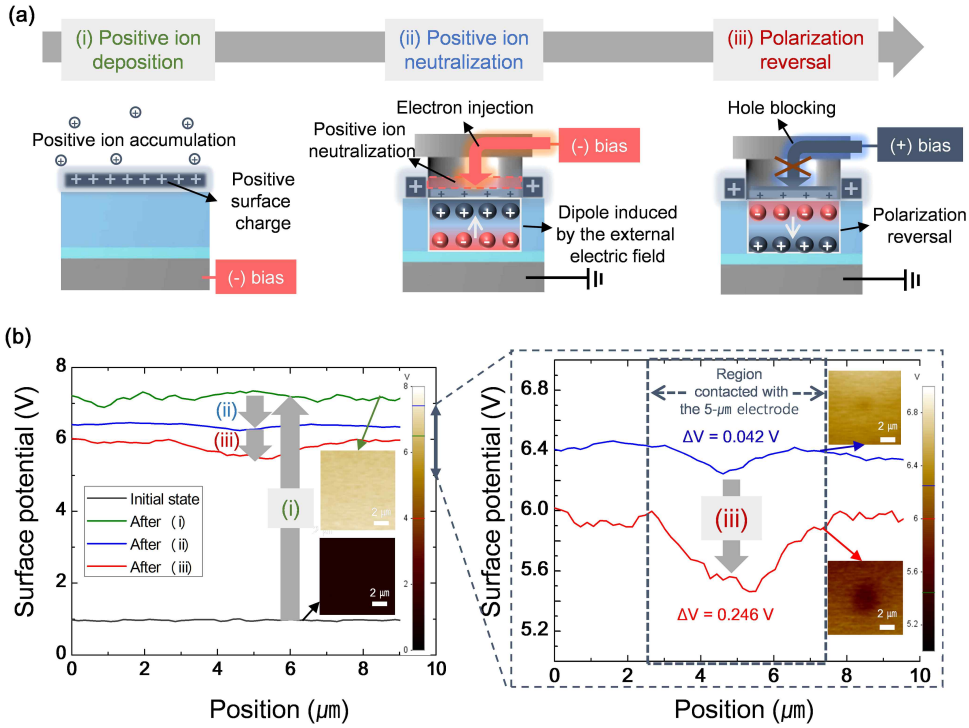

Figure 3.3 (a) Schematic illustration of detailed procedures for charge writings. (b) Surface potential data measured by KFM at the middle of the charge pattern (5 ㎛ in diameter) during each process. The inset shows the KFM image of the substrate at the end of each process.

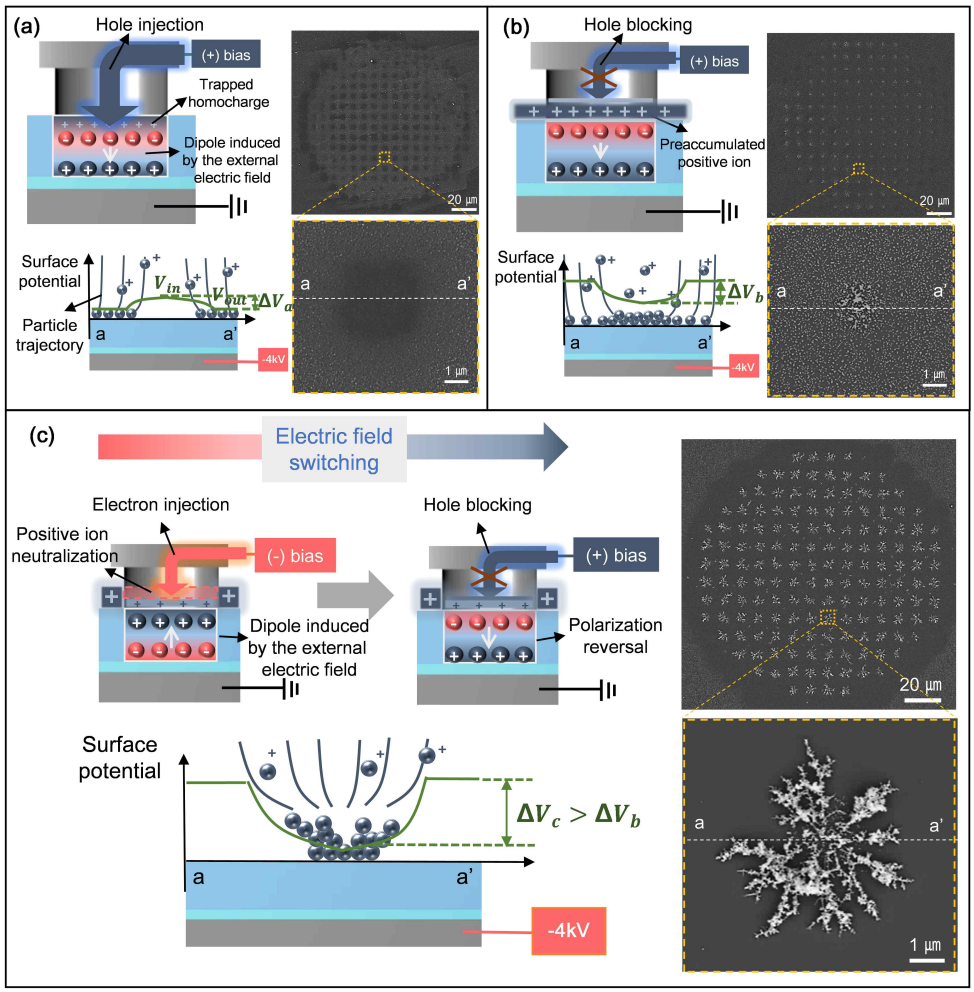

Figure 4.1 Schematic diagrams for the particle guiding and the fabricated assemblies according to three different approaches. (a) A conventional electrical contact under the positive bias. (b) An electrical contact under the positive bias on a positively charged surface. (c) Electrical contacts under the switched bias from negative to positive together with the employment of the positively charged surface.

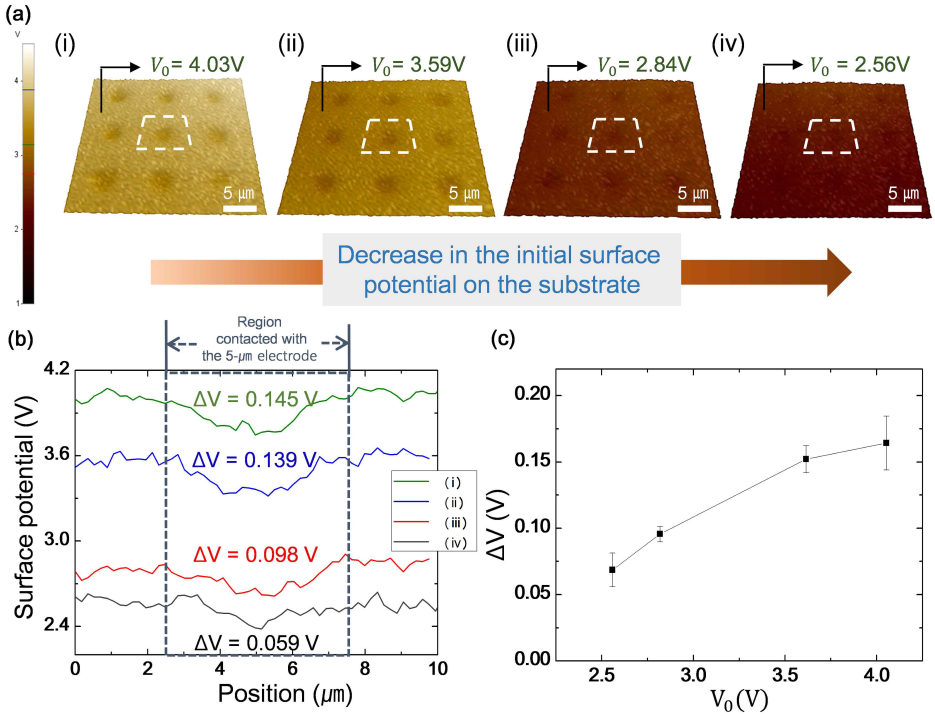

Figure 4.2. (a) KFM Images of the charge patterns produced from different values of the initial potentials increased by the positive ion deposition time. (b) Surface potential profiles of the four cases measured at the middle of each charged region from the white boxes in (a). (c) Plot of the potential differences of the charge patterns with the differently increased surface potential by the pre-accumulated positive ions.

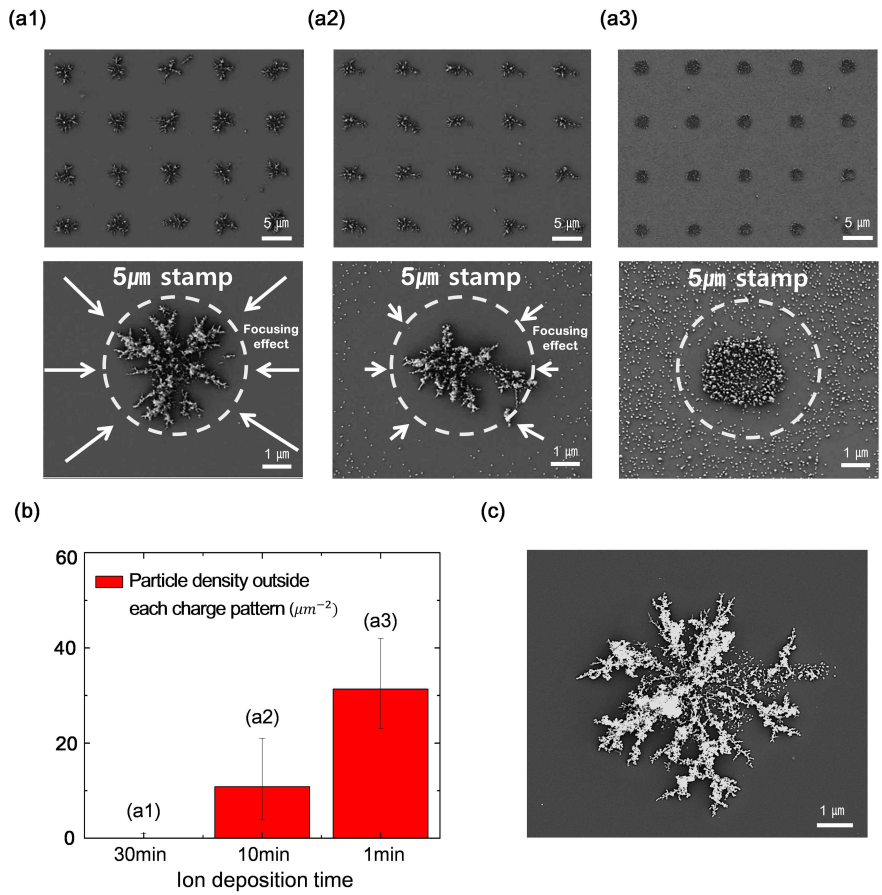

Figure 4.3 (a1−a3) SEM images of 40−nm silver nanoparticle pattern through the present approach with the different positive ion deposition time such as (a1) 30min, (a2) 10min and (a3) 1min. (b) Measured density of the noise particle located outside the charge pattern marked as circled regions. (c) A SEM image of the nanoparticle pattern through the present approach with the different positive ion deposition time of 1 hour

References

1. X. L. Ma, Z. Xie, Z. L. Liu, X. Q. Liu, T. B. Cao and Z. J. Zheng, *Adv Funct Mater*, 2013, **23**, 3239-3246.
2. G. M. Sessler and J. E. West, *J Acoust Soc Am*, 1966, **40**, 1433-1440.
3. M. Ignatova, T. Yovcheva, A. Viraneva, G. Mekishev, N. Manolova and I. Rashkov, *Eur Polym J*, 2008, **44**, 1962-1967.
4. P. P. Tsai, H. Schreuder-Gibson and P. Gibson, *J Electrostat*, 2002, **54**, 333-341.
5. M. Dreyer and R. Wiesendanger, *Appl Phys a-Mater*, 1995, **61**, 357-362.
6. H. O. Jacobs and G. M. Whitesides, *Science*, 2001, **291**, 1763-1766.
7. T. J. Krinke, K. Deppert, M. H. Magnusson and H. Fissan, *Part Part Syst Char*, 2002, **19**, 321-326.
8. R. Diaz, E. Palleau, D. Poirot, N. M. Sangeetha and L. Ressier, *Nanotechnology*, 2014, **25,** 345302.
9. L. S. McCarty, A. Winkleman and G. M. Whitesides, *Angew Chem Int Edit*, 2007, **46**, 206-209.
10. J. J. Cole, C. R. Barry, X. Y. Wang and H. O. Jacobs, *Acs Nano*, 2010, **4**, 7492-7498.
11. D. Zhao, L. T. Duan, M. Q. Xue, W. Ni and T. B. Cao, *Angew Chem Int Edit*, 2009, **48**, 6699-6703.

12. X. L. Xi, D. Zhao, F. Tong and T. B. Cao, *Soft Matter*, 2012, **8**, 298-302.
13. H. Fudouzi, M. Kobayashi and N. Shinya, *Adv Mater*, 2002, **14**, 1649-1652.
14. J. U. Park, S. Lee, S. Unarunotai, Y. G. Sun, S. Dunham, T. Song, P. M. Ferreira, A. G. Alleyne, U. Paik and J. A. Rogers, *Nano Lett*, 2010, **10**, 584-591.
15. W. L. W. Hau, D. W. Trau, N. J. Sucher, M. Wong and Y. Zohar, *J Micromech Microeng*, 2003, **13**, 272-278.
16. M. Kang, H. Kim, B. W. Han, J. Suh, J. Park and M. Choi, *Microelectron Eng*, 2004, **71**, 229-236.
17. D. Zhao, J. X. Peng, X. F. Tang, D. D. Zhang, X. H. Qiu, Y. L. Yang, Y. P. Wang, M. N. Zhang, L. Guan and T. B. Cao, *Soft Matter*, 2013, **9**, 9702-9708.
18. E. Palleau, N. M. Sangeetha, G. Viau, J. D. Marty and L. Ressier, *Acs Nano*, 2011, **5**, 4228-4235.
19. P. Moutet, N. M. Sangeetha, L. Ressier, N. Vilar-Vidal, M. Comesana-Hermo, S. Ravaine, R. A. L. Vallee, A. M. Gabudean, S. Astilean and C. Farcau, *Nanoscale*, 2015, **7**, 2009-2022.
20. L. Ressier and V. Le Nader, *Nanotechnology*, 2008, **19,** 135301.
21. E. Palleau, N. M. Sangeetha and L. Ressier, *Nanotechnology*, 2011, **22,** 325603.
22. M. Ieda, *Ieee T Electr Insul*, 1980, **15**, 206-224.

23. J. J. Cole, E. C. Lin, C. R. Barry and H. O. Jacobs, *Appl Phys Lett*, 2009, **95,** 113101.
24. P. Maksymovych, S. Jesse, P. Yu, R. Ramesh, A. P. Baddorf and S. V. Kalinin, *Science*, 2009, **324**, 1421-1425.
25. A. Gruverman, D. Wu, H. Lu, Y. Wang, H. W. Jang, C. M. Folkman, M. Y. Zhuravlev, D. Felker, M. Rzchowski, C. B. Eom and E. Y. Tsymbal, *Nano Lett*, 2009, **9**, 3539-3543.
26. H. Park, H. Cho, J. Kim, J. W. Bang, S. Seo, Y. Rahmawan, D. Y. Lee and K. Y. Suh, *Small*, 2014, **10**, 52-59.
27. H. Cho, J. Kim, H. Park, J. W. Bang, M. S. Hyun, Y. Bae, L. Ha, D. Y. Kim, S. M. Kang, T. J. Park, S. Seo, M. Choi and K. Y. Suh, *Nat Commun*, 2014, **5,** 3137.
28. H. Cho, J. Kim, K. Suga, T. Ishigami, H. Park, J. W. Bang, S. Seo, M. Choi, P. S. Chang, H. Umakoshi, S. Jung and K. Y. Suh, *Lab Chip*, 2015, **15**, 373-377.
29. K. Lim, J. R. Lee, H. Lee, P. V. Pikhitsa, S. You, C. G. Woo, P. Kim, K. Y. Suh and M. Choi, *Appl Phys Lett*, 2012, **101,** 203106.
30. H. Kim, J. Kim, H. J. Yang, J. Suh, T. Kim, B. W. Han, S. Kim, D. S. Kim, P. V. Pikhitsa and M. Choi, *Nat Nanotechnol*, 2006, **1**, 117-121.
31. K. Jung, H. J. Song, G. Lee, Y. Ko, K. Ahn, H. Choi, J. Y. Kim, K. Ha, J. Song, J. K. Lee, C. Lee and M. Choi, *Acs*

Nano, 2014, **8**, 2590-2601.

32. Y. Li and T. Takada, *J Phys D Appl Phys*, 1992, **25**, 704-716.

33. Z. Ziari, S. Sahli, A. Bellel, Y. Segui and P. Raynaud, *Ieee T Dielect El In*, 2011, **18**, 1408-1415.

나노제로그래피 기술 향상을 위한 양하전된 절연체 위에서의 전기장 반전 과정에 대한 분석

서울대학교 대학원
기계항공공학부
이 해 욱

요 약

본 논문은 양하전된 절연체 위에 접촉되어 있는 전극에 걸어주는 전압을 반전시키는 과정을 통하여 기존의 나노제로그래피 공정에서 사용된 것보다 훨씬 낮은 세기의 전기장(< 3.3 V/㎛)을 사용하였음에도 불구하고 강력한 집속력을 가지는 하전 패턴을 생성시킬 수 있는 새로운 방법을 제시하였다. 전극에 가해진 전압을 음극에서 양극으로 반전시키는 과정동안 이루어지는 두 번의 전기적 접촉 과정에서 전극으로부터 주입되는 전자와 정공은 미리 절연체에 형성되어 있는 양극의 표면 전하로 인하여 비대칭적으로 조절되도록 하였으며 이를 통하여 각각의 과정동안 하전 패턴이 다른 매커니즘을 통하여 생성될 수 있도록 하였다. 본 논문에서 제시된 방법을 증명하기 위해, Kelvin Force Microscopy (KFM) 장비를 통해 측정된 표면 전압 값과 양극 하전된 나노 입자를 하전 패턴을 통하여 집속시키는 실험을 수행하였으며 또한 금속이 코팅된 계층 폴리머 전극을 사용함으로써 기판과 밀접하게 접촉할 수 있도록 하여 균일한 하전 패턴을 생성시킬 수 있도록 하였다. 그 결과, 기존의 나노제로

그래피에서 사용된 것보다 훨씬 낮은 값의 전기장을 가해주었음에도 불구하고 전기적 접촉과정 이전에 형성시킨 표면 전압의 값을 증가시키는 방법을 통하여 최종적으로 매우 강력한 집속력을 가지는 하전 패턴을 생성시킬 수 있음을 확인하였으며 이를 통해 기존의 나노제로그래피로 생성시킨 하전 패턴의 한계를 넘어서는 집속력을 가질 수 있음을 증명하였다.

주 요 어 : Nanoxerography, Electric Field Switching, Corona Charging, Dielectric, Charge Pattern, Nanoparticle Pattern

학번 : 2013-23835